

## Mo marine geochemistry and reconstruction of ancient ocean redox states

CHENG Meng<sup>1,2</sup>, LI Chao<sup>2\*</sup>, ZHOU Lian<sup>3</sup> & XIE ShuCheng<sup>2</sup>

<sup>1</sup> School of Earth Sciences, China University of Geosciences, Wuhan 430074, China;

<sup>2</sup> State Key Laboratory of Biogeology and Environmental Geology, China University of Geosciences, Wuhan 430074, China;

<sup>3</sup> State Key Laboratory of Geological Processes and Mineral Resources, China University of Geosciences, Wuhan 430074, China;

Received March 30, 2015; accepted July 24, 2015

Molybdenum (Mo) proxies, including bulk concentration and isotopic composition, have been increasingly used to reconstruct ancient ocean redox states. This study systematically reviews Mo cycles and their accompanying isotopic fractionations in modern ocean as well as their application in paleo-ocean redox reconstruction. Our review indicates that Mo enrichment in sediments mainly records the adsorption of Fe-Mn oxides/hydroxides and chemical bonding of H<sub>2</sub>S. Thus, Mo enrichment in anoxic sediments generally reflects the presence of H<sub>2</sub>S in the water column or pore waters. In addition to the effect of euxinia, sedimentary Mo enrichment is related to the size of the oceanic Mo reservoir. Given these primary mechanisms for oceanic Mo cycling, Mo abundance data and Mo/TOC ratios acquired from euxinic sediments in geological times show that fluctuations of the oceanic Mo reservoir are well correlated with oxygenation of the atmosphere and oceans and suggest that oxygenation occurred in phases. Mo proxies suggest that Mo isotopes in strongly euxinic sediments reflect the contemporaneous Mo isotopic composition of seawater, but other processes such as iron-manganese (Fe-Mn) adsorption and weak euxinia can result in different fractionations. Diagenesis may complicate Mo enrichment and its isotopic fractionation in sediments. With appropriate constraints on the Mo isotopic composition of seawater and various outputs, a Mo isotope mass-balance model can quantitatively reconstruct global redox conditions over geological history. In summary, Mo proxies can be effectively used to reconstruct oceanic redox conditions on various timescales due to their sensitivity to both local and global marine redox conditions. However, given the complexity of geochemical processes, particularly the effects of diagenesis, further work is required to apply Mo proxies to ancient oceans.

### Mo enrichment, Mo isotopic fractionation, Mo isotope mass-balance model, ancient ocean chemistry

**Citation:** Cheng M, Li C, Zhou L, Xie S C. 2015. Mo marine geochemistry and reconstruction of ancient ocean redox states. *Science China: Earth Sciences*, 58: doi: 10.1007/s11430-015-5177-4

Studies of ancient ocean chemistry aim to reconstruct the water chemistry and spatial redox structures in a given period as well as their evolution over geological time. To accomplish this goal, numerous geochemical proxies have been proposed, including Fe-S-C-N (e.g., Lyons et al., 2009), biomarkers such as alkane and sterane (e.g., Brocks, 2005), and the concentrations and isotopic compositions of

redox-sensitive elements such as Mo, V, Cr, U, and Se (e.g., Algeo and Maynard, 2004; Anbar and Rouxel, 2007), all of which have advanced understanding of ancient ocean chemistry. Recently, new hot topics have emerged in this research, for example, quantitative analysis of both ocean chemistry and seawater sulfate concentration (Kah et al., 2004; Loyd et al., 2012) and characterization of the high spatial heterogeneity of ocean chemistry (Feng et al., 2014; Li et al., 2010; Poulton et al., 2010). These research direc-

\*Corresponding author (email: chaoli@cug.edu.cn)

tions demand both sensitive and quantitative geochemical proxies for ancient ocean chemistry reconstruction.

Analytical methods for many non-traditional stable isotopes, particularly transition metals, have been well developed in the past decade, benefitting from the great progress in isotopic double-spike and sample separation-purification techniques. Currently, accurate isotopic analysis is possible for elements including Mo, V, Cr, U, Se, etc., allowing their application in the reconstruction of ancient ocean chemistry. Of these elements, Mo has received increasing attention because of its high sensitivity to water redox conditions. However, the complexity of Mo's geochemical cycle and its accompanying isotopic fractionations in the ocean still pose significant challenges. In this paper, we review the latest progress and important breakthroughs in Mo geochemical theories and their applications in paleo-ocean redox reconstruction. We emphasize the Mo cycle and Mo isotopic fractionation in modern and ancient oceans, which will inform the use of Mo proxies in paleo-ocean redox reconstruction.

## 1 Mo marine geochemical cycle and sedimentary enrichment

Mo has concentrations of approximately 1–2 ppm in the upper continental crust (Turekian and Holland, 2013) and is mainly found as  $\text{MoS}_2$  or as  $\text{PbMoO}_4$  or  $\text{CaMoO}_4$  with relatively high concentrations in magmatic accessory minerals (e.g., apatite and titanite) (Miller et al., 2011). Oceanic Mo mainly originates from riverine flux, which has an average concentration of 6 nmol/L (Archer and Vance, 2008) and totals  $2.6 \times 10^8$ – $3.1 \times 10^8$  mol yr<sup>-1</sup> (Miller et al., 2011; Rahaman et al., 2010). Given the low concentration of Mo in continental crust, linear correlation between Mo and sulfate concentrations in river water suggests that riverine Mo is probably sourced from weathering of pyrite-bearing rocks (Archer and Vance, 2008; Miller et al., 2011). Mo concentrations in low temperature hydrothermal fluids are several times higher than in seawater but provide only 10%–14% of riverine Mo flux to the ocean (McManus et al., 2002; Wheat et al., 2002). The valence state of Mo (+2, +3, +4, +5, or +6) varies depending on pH and oxygen levels (Anbar, 2004). Mo is present in oxic seawater as  $\text{MoO}_4^{2-}$  with a concentration of 107 nmol/L, which has the highest concentration of the transition elements. The residence time of Mo in the modern ocean is 0.44–0.7 Ma, which is much longer than the average ocean mixing time of 1.5 kyr (Collier, 1985; Miller et al., 2011).

Except for a small amount of Mo that precipitates in high-temperature hydrothermal environments (Metz and Trefry, 2000), the export of Mo from the ocean is generally a function of oceanic redox conditions. In oxic bottom waters, Mo can be slowly adsorbed by manganese oxides/hydroxides (Mn-ox), yielding high Mo concentrations

in pelagic Fe-Mn nodules/crusts (Barling and Anbar, 2004). In anoxic bottom waters, aqueous  $\text{H}_2\text{S}$  can break the Mo=O bond, substituting S for O to form a series of thiomolybdate ions ( $\text{MoO}_{4-x}\text{S}_x^{2-}$ ,  $x=1-4$ ) and finally  $\text{MoS}_4^{2-}$  (Helz et al., 1996).  $\text{MoS}_4^{2-}$  may be further incorporated into sediments by combination with organic matter (Algeo and Lyons, 2006) or by forming Fe-S-Mo nano-minerals (Helz et al., 2011) and is finally converted into compounds with +4 valence (Dahl et al., 2010a; Wang et al., 2011). Thus, high sedimentary Mo concentrations generally reflect euxinic water conditions. A compilation of Mo abundance data for the modern ocean shows that the highest enrichment (>100 ppm) is associated with persistent euxinia, moderate enrichment (25–100 ppm) with intermittent euxinia, and weak enrichment (<25 ppm) with oxic/suboxic sediments (Scott and Lyons, 2012).

As described above, sedimentary Mo enrichment is generally controlled by the adsorption of Fe-Mn-ox in oxic/suboxic waters or the thio-effect of  $\text{H}_2\text{S}$  in euxinic waters (and/or pore waters). Thus, sedimentary Mo enrichment can serve as a powerful indicator of water redox conditions during deposition. For example, black shales generally have high Mo concentrations similar to those observed in the modern Black Sea, reflecting a euxinic water column. Likewise, high concentrations of Mo in sediments with extremely high Fe-Mn contents similar to those in modern pelagic Fe-Mn nodules/crusts reflect oxic water conditions during deposition. However, Mo enrichment becomes more complex when the chemocline approaches the water-sediment interface, when the water column and pore water redox conditions will differ. In this case, the amount of sedimentary Mo enrichment is related to the supply of organic matter and various oxides (Canfield and Thamdrup, 2009). The relatively high Fe-Mn deposition caused by oxic bottom waters may result in massive adsorption and precipitation of Mo. However, reduction of Fe-Mn-ox by organic matter can cause subsequent release of the adsorbed Mo into the pore waters (Morford et al., 2001). If  $\text{H}_2\text{S}$  is not present in pore waters, the re-released Mo will diffuse back to the overlying water column. If euxinia develops in the pore waters through bacterial sulfate reduction, the re-released Mo will be retained in the sediments. In sum, if Fe-Mn-ox adsorption does not occur, high sedimentary Mo enrichment should generally reflect a euxinic water column and/or pore waters.

In addition to water redox conditions, sedimentary Mo enrichments are also controlled by seawater Mo availability, which is related to basinal hydrology and the size of the oceanic Mo reservoir. Seawater Mo availability can be derived from Mo/TOC because Mo-enrichment effects can be evaluated based on TOC (Algeo and Lyons, 2006; Scott et al., 2008). For example, because the Mo reservoir in the early oceans was much smaller than in modern oceans, even euxinic sediments have low Mo concentrations and a low Mo/TOC ratio indistinguishable from continental crust

(Reinhard et al., 2009). Moreover, sedimentary Mo enrichment also has a good correlation with seawater exchange rates in modern euxinic basins with different-degree hydrological restrictions. Thus, comparison of Mo/TOC values from various tectonic environments can reflect the restriction degree of a basin at a given time (Algeo and Lyons, 2006), while the highest Mo/TOC values from open-water sediments should roughly reflect variations in the size of the global oceanic Mo reservoir through geologic time (Scott et al., 2008).

## 2 Temporal trends of sedimentary Mo abundance and Mo/TOC

The size of the oceanic Mo reservoir is essentially related to the oxygenation state of the atmosphere-ocean system. The temporal trends of Mo abundance and Mo/TOC in euxinic sediments can thus effectively record the evolution of the oceanic Mo reservoir, which further reflects the evolution of the oceanic redox state through geological time. Figure 1 summarizes the available sedimentary Mo abundance and Mo/TOC data from both euxinic and non-euxinic sediments in geological time. These data show high variability in the size of the oceanic Mo reservoir and two major oxygenation events for the atmosphere and ocean. Based on these two

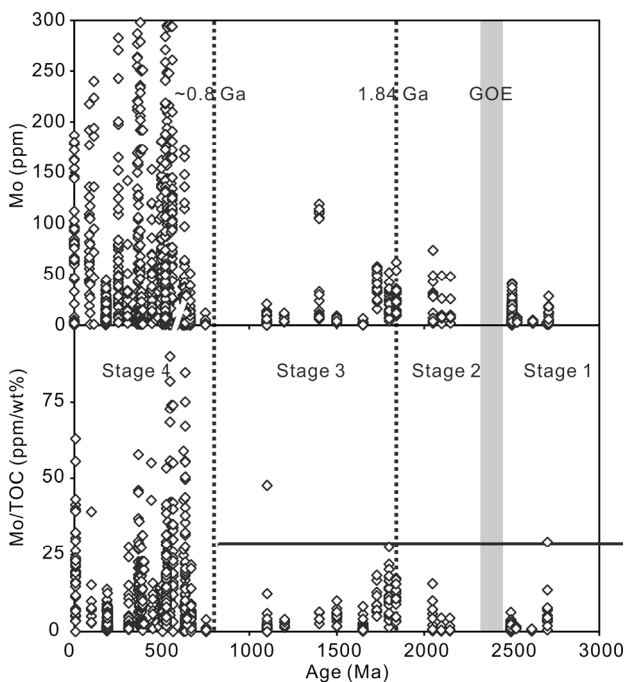


**Figure 1** Temporal trends in sedimentary Mo abundance and Mo/TOC values in geological time. Samples with Mo abundance in excess of 300 ppm or Mo/TOC in excess of 100 ppm/wt% are not shown. Data source: Chen et al. (2015), Feng et al. (2014), Gilleaudeau and Kah (2013), Goldberg et al. (2007), Kendall et al. (2015), Lehmann et al. (2007), Li et al. (2012, 2015), Scott et al. (2008) and references therein, Takahashi et al. (2014), Wen et al. (2015).

oxygenation events, the temporal record of Mo abundance can be roughly divided into four stages.

Stage 1 includes the period prior to the Great Oxidation Event (GOE, 2.45–2.32 Ga). At this stage, sediments generally have low Mo concentrations and low Mo/TOC values resembling the upper continental crust. For example, the 3.47 and 2.94 Ga black shales in Australia have Mo concentrations lower than 5 ppm, as do black shales in South Africa dated from 2.65 to 2.5 Ga (Wille et al., 2007, 2013). Although Mo concentrations are up to 50 ppm in the 2.5 Ga McRae black shales in Australia, the Mo/TOC values of these shales are only slightly higher than in the crust, consistent with a weak oxygenation event at this time (Duan et al., 2010; Reinhard et al., 2009). Mo concentrations and Mo/TOC values during stage 1 indicate that the Mo reservoir was much smaller than in the modern ocean, consistent with an extremely low oxygen level in the atmosphere-ocean system. Although oxygenic photosynthesis may have arisen earlier than the GOE, the oxygen level still remained low during this stage (Kasting, 2001).

Stage 2 covers the GOE to approximately 1.84 Ga. As a result of hydrogen escape and oxygenic photosynthesis (Kasting, 2001), a prominent increase in atmospheric oxygen occurred from 2.45–2.32 Ga after several whiffs of oxygenation events (Bekker et al., 2004; Canfield, 2005; Holland, 2006; Kump, 2008). Atmospheric oxygen concentrations may have exceeded 1% of the present atmospheric level (PAL) after the GOE (Farquhar, 2000). The subsequent Lomagundi carbon isotope excursion at approximately 2.1 Ga implies that the atmospheric oxygen level may have approached modern levels for a short time (Canfield et al., 2013). Correspondingly, Mo concentrations and Mo/TOC values in euxinic sediments from this stage are significantly higher than those of stage 1 (Figure 1).

Stage 3 occurs between 1.84 and 0.8 Ga. The increased atmospheric oxygen levels during the GOE may have not only directly oxygenated surface seawater (Slack and Cannon, 2009; Slack et al., 2007) but also caused the expansion of oceanic euxinia through increased input of sulfate from continental weathering (Poulton et al., 2010; Rouxel et al., 2005). This input may have been responsible for the disappearance of large-scale banded iron formations (BIFs) around 1.84 Ga (Canfield, 1998). Widespread euxinic waters in the middle Proterozoic may have caused drawdown of the global Mo reservoir, consistent with generally low sedimentary Mo concentrations and Mo/TOC values during this period (Scott et al., 2008). In addition, a recent study of chromium isotopes suggests a substantially low atmospheric oxygen level (as low as 0.1% PAL) (Planavsky et al., 2014b) existed during the Middle Proterozoic. This low oxygen level could be responsible for the small Mo reservoir during this period because it would correspond to a decrease in riverine input of oxidatively weathered Mo (Reinhard et al., 2013).

Stage 4 covers 0.8 Ga to the present. During the Neopro-

terozoic, the breakup of the Rodinia supercontinent involved significant tectonic activity (Li et al., 2008). In addition, the development of “Snowball Earth” indicates strong climatic turbulence at this time (Hoffman, 1998). A significant increase in atmospheric and oceanic oxygen levels may have occurred (Fike et al., 2006; McFadden et al., 2008; Och and Shields-Zhou, 2012; Sahoo et al., 2012), resulting in an expansion of the oceanic Mo reservoir. Therefore, significant elevation of sedimentary Mo concentrations and Mo/TOC values in euxinic sediments were recorded at this time (Figure 1). For example, the Mo reservoir may have reached modern levels shortly after the Marinoan glaciation (Sahoo et al., 2012), and a modern-like Mo marine cycle may have been established at approximately 551 Ma (Scott et al., 2008). In the Phanerozoic, because of widespread oxygenation of the atmosphere-ocean system, oceanic Mo concentrations generally remained high, as inferred from relatively high sedimentary Mo concentrations and Mo/TOC values (Scott et al., 2008).

We note that increasing evidence suggests high spatial heterogeneity in early ocean chemistry (e.g., Li et al., 2010; Poulton et al., 2010). It is not clear whether the Mo concentration was also spatially heterogeneous in the early ocean; if it occurred, this heterogeneity could have affected sedimentary enrichment of Mo. Thus, uncertainties may exist in reconstructions of ancient ocean chemistry, particularly if they rely on the record of sedimentary Mo abundance from a single site.

### 3 Mo isotopic fractionation and its applications

#### 3.1 Mo isotope terminology

Mo has seven stable isotopes, namely  $^{92}\text{Mo}$ ,  $^{94}\text{Mo}$ ,  $^{95}\text{Mo}$ ,  $^{96}\text{Mo}$ ,  $^{97}\text{Mo}$ ,  $^{98}\text{Mo}$  and  $^{100}\text{Mo}$ , with an average natural abundance of 14.84%, 9.25%, 15.92%, 16.68%, 9.55%, 24.13% and 9.63%, respectively (Anbar, 2004). In early studies, Mo isotope data were reported using  $\delta$  notation in per mille, following the equation  $\delta^{97}\text{Mo}$  ( $=[(^{97}\text{Mo}/^{95}\text{Mo})_{\text{sample}}/(^{97}\text{Mo}/^{95}\text{Mo})_{\text{standard}}-1]\times 1000$ ). Because of the wide application of the  $^{97}\text{Mo}$ - $^{100}\text{Mo}$  double spike in Mo isotopic analysis in recent years (Siebert et al., 2001), a new  $\delta$  notation has come into use, with the equation  $\delta^{98}\text{Mo}$  ( $=[(^{98}\text{Mo}/^{95}\text{Mo})_{\text{sample}}/(^{98}\text{Mo}/^{95}\text{Mo})_{\text{standard}}-1]\times 1000$ ). A simple approximation between the two notations is  $\delta^{97}\text{Mo}\approx 2/3\delta^{98}\text{Mo}$  (Anbar, 2004). Currently, there is no uniform Mo isotopic reference for data calibration, and different groups have used various laboratory references. The Mo plasma standard from the Johnson Matthey Company (JMC) and the mean ocean Mo (MOMO) are the two frequently used laboratory references. Relative to the former, modern seawater has an isotopic composition of +2.3‰. All Mo isotopic values discussed in this study are reported relative to the JMC reference standard. It should be noted that the Mo isotopic composition of

different batches of JMC standard are slightly different (<0.37‰) (Goldberg et al., 2013), so the batch number of the JMC standard used should be indicated when Mo isotopic data are reported.

#### 3.2 Mechanisms for Mo isotopic fractionation

In initial Mo isotope studies, based on a limited pool of Mo isotopic data that were mainly collected from magmatic and clastic rocks, the silicate crust was believed to have a homogeneous Mo isotopic composition of ~0‰ (Siebert et al., 2003). This value was widely used as the Mo isotopic composition of riverine flux into the ocean (Arnold et al., 2004; Wille et al., 2008). However, new studies of the Mo isotopic composition of global rivers suggest a variable  $\delta^{98}\text{Mo}$  value from +0.2‰ to +2.3‰ with an average of +0.7‰ (Archer and Vance, 2008), which is heavier than the Mo isotopic composition of upper continental crust. Other work has revealed that the rock types in a river’s catchment and drainage play an important role in determining the Mo isotopic composition of river water (Neubert et al., 2011). These findings led to a re-examination of Mo isotopic fractionation during magmatic processes. Voegelin et al. (2014) analyzed the Mo isotopic composition of a series of magmatic rocks ranging from olivine basalt to dacite, revealing an increase in  $\delta^{98}\text{Mo}$  values from +0.3‰ to +0.6‰ and in Mo concentrations from 0.8 to 4.1 ppm. This work indicates that high temperature magmatic processes indeed cause significant Mo isotopic fractionation. Thus, the average Mo isotopic composition of the upper continental crust was revised to the range from +0.3‰ to +0.6‰. Relative to the Mo isotopic compositions of upper continental crust and riverine flux, modern seawater has a homogeneous but highly positive Mo isotopic composition of +2.3‰. The difference between these values indicates that significant Mo fractionation must occur in the ocean. We summarize the currently known mechanisms below.

##### 3.2.1 Adsorption of Fe-Mn oxides/hydroxides

Mn oxides (Mn-ox) preferentially adsorb isotopically light Mo from seawater, causing a large fractionation of 3‰ from seawater Mo to adsorbed Mo (Barling and Anbar, 2004) that is supported by theoretical calculations and actual observations (Goldberg et al., 2012; Tossell, 2005). Because seawater temperature, salinity and other parameters have only limited effects on Mn-ox adsorption, this isotopic fractionation likely applies throughout geologic time (Wasylenki et al., 2008). Preferential adsorption of isotopically light Mo by iron oxides/hydroxides (Fe-ox) mainly occurs in dysoxic and ferruginous waters. When Mn-ox and Fe-ox coexist, Mo is adsorbed by Mn-ox instead of Fe-ox (Goldberg et al., 2009). The Mo isotopic fractionation caused by Fe-ox adsorption is a function of the iron mineral type: magnetite ( $\Delta^{98}\text{Mo}=0.83\text{‰}\pm 0.60\text{‰}$ )<ferrihydrite ( $\Delta^{98}\text{Mo}=1.11\text{‰}\pm 0.15\text{‰}$ )<goethite ( $\Delta^{98}\text{Mo}=1.40\text{‰}\pm 0.48\text{‰}$ )

<hematite ( $\Delta^{98}\text{Mo}=2.19\text{‰}\pm 0.54\text{‰}$ ) (Goldberg et al., 2009).

### 3.2.2 Thio-effect of $\text{H}_2\text{S}$

$\text{H}_2\text{S}$  in euxinic seawater plays an important role in Mo isotopic fractionation between seawater and sediments. Laboratory experiments indicate that the chemical behavior of Mo in  $\text{H}_2\text{S}$ -bearing systems is linked to a “geochemical switch” at approximately  $11\pm 3\ \mu\text{mol/L}$  (Helz et al., 1996). When the  $\text{H}_2\text{S}$  content of the water column is lower than the threshold value,  $\text{MoO}_4^{2-}$  can only be converted into  $\text{MoO}_{4-x}\text{S}_x^{2-}$  ( $x=1-3$ ), causing a large isotopic fractionation of  $0.7\text{‰}$  to  $3\text{‰}$  between seawater and sediments (Neubert et al., 2008). If  $\text{H}_2\text{S}$  only exists in pore waters, a roughly constant fractionation of  $0.7\text{‰}$  results (Poulson et al., 2006), although the mechanism behind this fractionation remains unclear. It may be related to mixing of Mo from different sources (Poulson et al., 2009). In contrast, when the  $\text{H}_2\text{S}$  content is higher than the threshold value,  $\text{MoO}_4^{2-}$  can be completely converted into  $\text{MoS}_4^{2-}$ . If complete precipitation of  $\text{MoS}_4^{2-}$  occurs, no fractionation will be observed between seawater and sediments; otherwise, a fractionation of up to  $0.5\text{‰}$  may occur (Nägler et al., 2011).

### 3.2.3 Biological activity

Although Mo is an essential nutrient for organisms (Liermann et al., 2005; Morel and Price, 2003), biological utilization seems to have only a minor effect on Mo isotopic composition in seawater (Brumsack, 1989). This is probably because the amount of Mo used by organisms is much smaller than in their environment (Nameroff et al., 2002). A recent study found that significant Mo isotopic fractionation occurred in the process of Mo transfer within cyanobacterial cells (Zerkle et al., 2011); however, this should have little influence on Mo fractionation in the open ocean (Kowalski et al., 2013). Anbar and Knoll (2002) argued that depletion of Mo in euxinic mid-Proterozoic oceans may have delayed eukaryotic evolution because Mo plays a key role in biological  $\text{N}_2$  fixation. Given the small Mo reservoir in early oceans, biological activity could have had a stronger influence on Mo isotopic fractionation than in the modern ocean, but this idea requires further investigation.

### 3.2.4 Diagenesis

Research on Mo isotopic fractionation during diagenesis is relatively limited. Along with mineralization of organic matter during diagenesis, Fe-Mn-ox is re-reduced and adsorbed Mo is subsequently released into pore waters or the overlying water column (Reitz et al., 2007). The behavior of Mo in pore waters is similar to that in the water column and depends on water redox conditions. Four cases of Mo behavior and corresponding isotopic fractionations were summarized by Scott and Lyons (2012) (Figure 2). (1) When bottom waters have high oxygen levels ( $\gg 10\ \mu\text{mol/L}$ ) and little organic matter is retained in the underlying sediment (Figure 2(a)), there will be high Mo concen-

tration in pore waters due to Mn-ox reduction and the release of adsorbed Mo. The released Mo will eventually return to the overlying water column, so that the Mo isotopic composition of the sediment is not affected. (2) When bottom waters have moderate oxygen levels ( $>10\ \mu\text{mol/L}$ ) and a moderate amount of organic matter is retained in the underlying sediment (Figure 2(b)), high Mo concentration may occur near the sediment surface due to Mn-ox reduction and the release of adsorbed Mo. Mo diffusing into lower pore waters can be trapped by pore-water  $\text{H}_2\text{S}$ , thus imparting a lower  $\delta^{98}\text{Mo}$  value to the sediments (Herrmann et al., 2012; Reitz et al., 2007). (3) When bottom waters have low oxygen levels ( $<10\ \mu\text{mol/L}$ ) and  $\text{H}_2\text{S}$  is present in pore waters (Figure 2(c)), the effect of Mn-ox on Mo cycling disappears. Sedimentary Mo enrichment is only associated with  $\text{H}_2\text{S}$  but is commonly less than 25 ppm (Scott and Lyons, 2012). In this case, the Mo isotopic fractionation between seawater and sediments is consistent at  $0.7\text{‰}$  (Poulson et al., 2006). (4) When bottom waters and sediments both have high  $\text{H}_2\text{S}$  concentrations, the sedimentary Mo enrichment is usually greater than 25 ppm (Scott and Lyons, 2012), and Mo isotopic compositions of sediments resemble overlying euxinic waters. The four cases described above involve transitions between redox conditions and possible superposition of multiple geochemical processes. Thus, Mo behavior is more complex in pore waters than in the water column and may result in abnormal sedimentary Mo isotopic compositions.

## 3.3 Applications of specific Mo isotopic fractionation mechanisms in ancient ocean chemistry reconstruction

As discussed above, sedimentary Mo isotopic compositions ( $\delta^{98}\text{Mo-sd}$ ) are strongly related to depositional redox conditions. Therefore,  $\delta^{98}\text{Mo-sd}$  values can serve as a powerful proxy for tracking ancient ocean redox conditions and evolution.

### 3.3.1 Fractionations related to Mn-ox adsorption

The formation of Mn-ox is a microbial process that depends

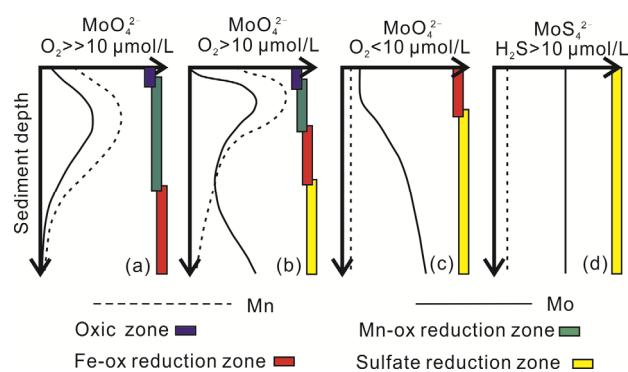


**Figure 2** Schematic of Mo cycling in sediments modified from Scott and Lyons (2012).

on the presence of free dissolved oxygen (Hansel et al., 2012). Therefore,  $\delta^{98}\text{Mo}$ -sd caused by Mn-ox adsorption can serve as evidence for the presence of free dissolved oxygen in early oceans. Although the mass independent fractionation (MIF) of sulfur isotopes provides strong evidence for a substantial increase in oxygen in the 2.45–2.32 Ga atmosphere-ocean system (Farquhar, 2000), little is known about the earth's redox state before the GOE. Based on the fractionation caused by Mn-ox formation,  $\delta^{98}\text{Mo}$ -sd records indicate that multiple weak oxygenations of the atmosphere-ocean system happened prior to the GOE (Czaja et al., 2012; Duan et al., 2010; Eroglu et al., 2015; Kurzweil et al., 2015; Wille et al., 2007). Planavsky et al. (2014a) found a good linear relationship between  $\delta^{98}\text{Mo}$  values and the Fe/Mn ratio for the >2.95 Ga BIF and therefore argued that photosynthetic oxygen began to accumulate in shallow marine settings no later than 2.95 Ga.

### 3.3.2 Fractionations related to Fe-ox adsorption

The Mo isotopic fractionation associated with Fe-ox adsorption is determined by the types of Fe-bearing minerals that are present (Goldberg et al., 2009). In natural environments, mixing of various Fe-bearing minerals results in complex Mo isotopic fractionations. Baldwin et al. (2013) obtained a  $\delta^{98}\text{Mo}$  value of +0.7‰ from a <716 Ma IF. As the iron in the IF mainly presented as hematite, a laboratory-inferred fractionation of 1.1‰ between hematite-adsorbed Mo and seawater (Goldberg et al., 2009) indicates that the contemporaneous seawater Mo isotopic composition was +1.8‰, which suggests significant oxygenation of the late Neoproterozoic ocean. However, Mo isotope data from 750 Ma black shales suggests a seawater  $\delta^{98}\text{Mo}$  value of +1.1‰ (Dahl et al., 2011) with no evidence for significant oxygenation of the ocean between 750 Ma and 716 Ma. Experiments by Goldberg et al. (2009) showed a strong effect of pH on Mo isotopic fractionation during adsorption of Mo onto Fe-ox, which may help to explain the heavy sedimentary  $\delta^{98}\text{Mo}$  value acquired from the <716 Ma IF. In addition, if the Mo reservoir at this time was much smaller than in the modern ocean, the  $\delta^{98}\text{Mo}$ -sw value might be more sensitive to the influence of Fe-ox adsorption than in the modern ocean (Kendall et al., 2015). Thus, the  $\delta^{98}\text{Mo}$  value from the IF could be poorly representative of the oceanic redox state. Obviously, more work is needed to use the Fe-ox adsorption-related Mo isotopic fractionation in reconstruction of paleo-ocean redox conditions.

### 3.3.3 Fractionations related to $\text{H}_2\text{S}$

In weakly euxinic conditions ( $[\text{H}_2\text{S}]_{\text{aq}} < 11 \mu\text{mol/L}$ ),  $\text{MoO}_4^{2-}$  cannot be completely converted to  $\text{MoS}_4^{2-}$ , resulting in significant isotopic fractionation (Helz et al., 1996). The  $\text{H}_2\text{S}$  concentration of the modern Black Sea increases from zero at the 110-m chemocline to approximately 11  $\mu\text{mol/L}$  at 400 m, while the sedimentary  $\delta^{98}\text{Mo}$  values increase linearly from -0.7‰ to the modern seawater composition of +2.3‰

(Neubert et al., 2008). Using this relationship between the  $\text{H}_2\text{S}$  concentration and the  $\delta^{98}\text{Mo}$ -sw value, Arnold et al. (2012) reconstructed the evolution of  $\text{H}_2\text{S}$  concentrations in the Black Sea over the past 300 years. This work represents the first quantitative analysis of the  $\text{H}_2\text{S}$  concentration in ancient oceans. Although rare in the modern ocean, euxinic waters occur frequently in the geologic record (Feng et al., 2014; Li et al., 2010, 2012; Poulton et al., 2010), where it can be identified by using geochemical proxies such as iron speciation and concentrations of redox-sensitive elements (Lyons et al., 2009). Measuring the  $\delta^{98}\text{Mo}$  value of these strongly euxinic sediments should allow reconstruction of the contemporaneous seawater Mo isotopic composition. In the modern ocean, the residence time of Mo is much greater than the ocean mixing time (Miller et al., 2011), so the global seawater has a uniform Mo isotopic composition. If we constrain the Mo residence time by using Mo/TOC values (Algeo, 2004) and assume that the ancient seawater  $\delta^{98}\text{Mo}$  value was homogeneous at a given time, a Mo-isotope mass balance model that incorporates  $\delta^{98}\text{Mo}$  values from strongly euxinic sediments should be able to calculate the global oceanic redox state (see Section 4). Arnold et al. (2004) employed this concept to explore global redox conditions in the mid-Proterozoic ocean and found that anoxic water conditions prevailed at that time. Although the oceanic Mo budget framework in Arnold et al. (2004) is oversimplified (Kendall et al., 2009), the idea has since been widely applied to other geological periods including the late Paleoproterozoic (Kendall et al., 2011), early Paleoproterozoic (Siebert et al., 2005), Neoproterozoic (Dahl et al., 2011), early Cambrian (Chen et al., 2015; Wille et al., 2008) and Phanerozoic (Pearce et al., 2008; Proemse et al., 2013). By compiling  $\delta^{98}\text{Mo}$ -sw values over time, it is possible to reconstruct the global evolution of oceanic redox state. For example, Dahl et al. (2010b) compiled  $\delta^{98}\text{Mo}$ -sw values with ages <1.8 Ga and found that  $\delta^{98}\text{Mo}$ -sw values approached modern in the Devonian, which in turn suggests that the ocean was not fully oxygenated until the Devonian.

## 4 Mo isotope mass-balance model

A Mo isotope mass-balance model is used for quantitative reconstruction of the global oceanic redox state.

### 4.1 Basic components of the model

Seawater will have a uniform isotopic composition if the Mo residence time in the ocean is longer than the seawater mixing time. Under this circumstance, any strongly euxinic sediment should record the contemporaneous seawater isotopic composition, thus yielding information about the global oceanic redox state. A “one-box” model is usually used for this isotope mass-balance calculation for a steady state ocean (Kendall et al., 2009; Figure 3). A typical equa-

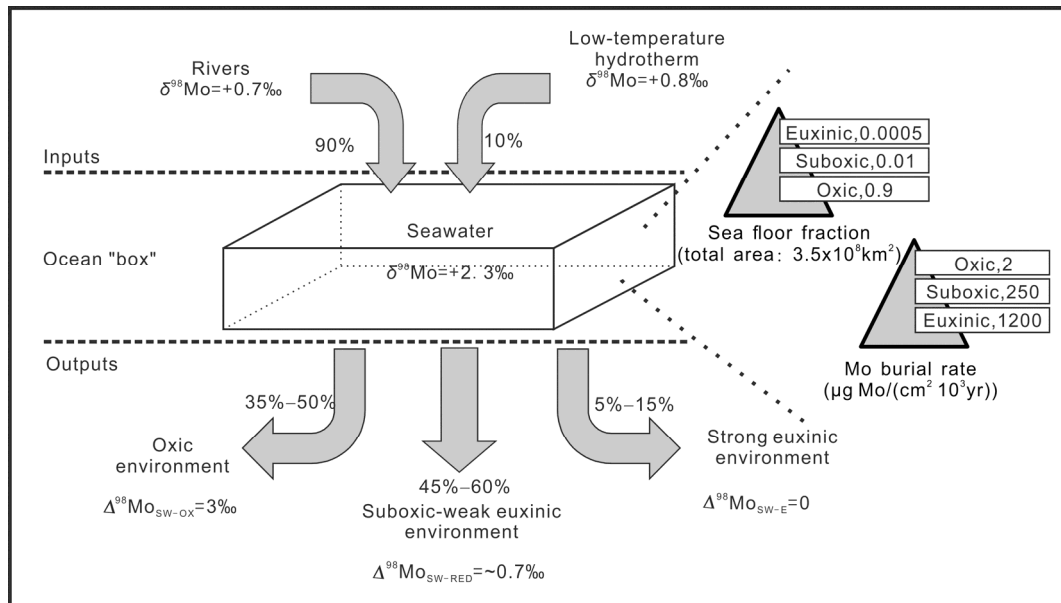


**Figure 3** Schematic presentation of Mo isotope mass-balance model for the modern ocean. Data source: Archer and Vance (2008), Barling and Anbar (2004), Barling et al. (2001), Dahl et al. (2010b), Kendall et al. (2009), McManus et al. (2002), Poulson et al. (2009), Siebert et al. (2003).

tion is given below:

$$F_R \delta_R + F_{LTH} \delta_{LTH} = F_O \delta_O + F_{RED} \delta_{RED} + F_E \delta_E, \quad (1)$$

where  $F$ , Mo flux; R, rivers; LTH, low-temperature hydrothermal environments; O, oxic environments; RED, suboxic, ferruginous and weakly euxinic environments ( $[\text{H}_2\text{S}]_{\text{aq}} < 11 \mu\text{mol/L}$ ); and E, strongly euxinic environments ( $[\text{H}_2\text{S}]_{\text{aq}} > 11 \mu\text{mol/L}$ ).

The left side of eq. (1) represents Mo inputs to the ocean by rivers and low-temperature hydrothermal activity. Riverine Mo provides more than 90% of inputs, while LTH provides less than 10% (Figure 3). Climate and rock type in the source area have major effects on the  $\delta^{98}\text{Mo}$  value of river water (Neubert et al., 2011), and modern riverine Mo has an average  $\delta^{98}\text{Mo}$  value of  $+0.7\text{‰}$  (Archer and Vance, 2008). However, on geologic timescales, especially in the Precambrian, when the atmospheric oxygen level was significantly lower than today, the riverine Mo could have had a different isotopic composition from today. Some researchers have argued that the past riverine  $\delta^{98}\text{Mo}$  value was between  $0$ – $+0.7\text{‰}$  (Xu et al., 2012), whereas others have argued for a stable isotopic composition throughout geologic time (Hannah et al., 2007). Mo sourced from LTH was generally considered to have an isotopic composition of  $+0.8\text{‰}$  (McManus et al., 2002), which is slightly higher than the upper crustal  $\delta^{98}\text{Mo}$  value. Given the small hydrothermal contribution of Mo to the ocean, its influence on the Mo isotope mass balance is likely limited. However, it should not be ignored during periods when hydrothermal activity was high (Kump and Seyfried, 2005) and may have had a different isotopic composition from modern hydrothermal Mo (Greber et al., 2011).

The right side of eq. (1) represents the  $\delta^{98}\text{Mo}$  value of Mo outputs from the ocean under different water redox conditions, including oxic, suboxic-weakly euxinic and strongly euxinic environments. When a sample deposits under strongly euxinic conditions ( $[\text{H}_2\text{S}] > 11 \mu\text{mol/L}$ ), the sedimentary  $\delta^{98}\text{Mo}$  value should be equivalent to the seawater  $\delta^{98}\text{Mo}$  value (Arnold et al., 2004). The  $\delta^{98}\text{Mo}$  value of the oxic sediments (i.e.,  $\delta_O$ ) can be constrained as  $\delta = \delta_E - 3\text{‰}$  given the 3‰ fractionation for Mo between seawater and sediments under oxic conditions that takes place by Mn-ox adsorption (Wasylenki et al., 2008). Because authigenic Mo precipitating in euxinic pore waters experiences a 0.7‰ fractionation from seawater (Poulson et al., 2006, 2009), the resulting sedimentary  $\delta^{98}\text{Mo}$  value ( $\delta_{\text{aug}}$ ) can be similarly estimated as  $\delta_{\text{aug}} = \delta_E - 0.7\text{‰}$ . Sediments deposited in RED always show a large fractionation relative to seawater; this value is usually simplified to  $\delta_{\text{aug}}$  via the equation  $\delta_{\text{RED}} = \delta_E - 0.7\text{‰}$ . Studies of the modern ocean indicate that the fractions of Mo removed from oxic, RED and strongly euxinic waters are estimated to be 35%–50%, 5%–15% and 45%–60%, respectively (Dahl et al., 2010b; Kendall et al., 2009; Scott et al., 2008).

#### 4.2 Approaches and problems for seawater Mo isotope reconstruction

Because the isotopic composition of each Mo sink is estimated from the contemporaneous seawater  $\delta^{98}\text{Mo}$  value, an accurate reconstruction of the seawater  $\delta^{98}\text{Mo}$  value over time is crucial to quantifying past oceanic redox conditions. The fact that black shales with high organic matter concentrations are usually considered to be deposited under euxinic

water conditions (Lyons et al., 2009) provides an approach for estimation of seawater Mo isotopic compositions over geologic time. Most studies of seawater Mo isotopic composition have therefore focused on black shales (Arnold et al., 2004; Pearce et al., 2008). However, not all black shales deposited under euxinic water conditions (Gordon et al., 2009), and even when aqueous  $\text{H}_2\text{S}$  concentrations exceed  $11 \mu\text{mol/L}$ , a weak fractionation of up to  $0.5\text{‰}$  could still exist between the sediments and the seawater due to incomplete deposition of Mo (Nägler et al., 2011). Using black shales to calculate the global seawater  $\delta^{98}\text{Mo}$  value also assumes that the seawater  $\delta^{98}\text{Mo}$  value is uniform at a given time. Essentially, this would require a large enough oceanic Mo reservoir to sustain a Mo residence time longer than the oceanic mixing time. High  $\text{H}_2\text{S}$  concentrations in the water column ensure that underlying sediments faithfully record the seawater  $\delta^{98}\text{Mo}$  value, but if euxinia were globally widespread, Mo outputs could exceed Mo inputs to the ocean. These conditions would significantly reduce the size of the Mo reservoir and could make the  $\delta^{98}\text{Mo}$ -sw value spatially heterogeneous (Wen et al., 2011). Thus, an isotope mass balance model using local  $\delta^{98}\text{Mo}$  values to predict the global  $\delta^{98}\text{Mo}$ -sw value would no longer be valid. We also note that the sporadic occurrence of strongly euxinic black shales in the geologic record means that this approach may only provide a discontinuous record of the  $\delta^{98}\text{Mo}$ -sw value.

Marine carbonates generally have a Mo concentration below 1 ppm, and carbonate-associated Mo precipitation accounts for only  $\leq 1\%$  of global oceanic Mo output (Voegelin et al., 2009). The  $\delta^{98}\text{Mo}$  value of modern oceanic carbonates has been shown to track the  $\delta^{98}\text{Mo}$ -sw value and thus could serve as an indicator for the Mo isotopic composition of seawater (Voegelin et al., 2009). Compared to strongly euxinic black shales, carbonates are more continuous through geologic time, making reconstruction of  $\delta^{98}\text{Mo}$ -sw values from carbonates promising (Voegelin et al., 2010). However, because Mo concentrations in carbonates are very low, the carbonate-associated Mo can be easily masked by terrigenous Mo, so that a calibration of terrigenous Mo is necessary (Voegelin et al., 2010; Voegelin et al., 2009). Similarly, phosphorite deposits can also record  $\delta^{98}\text{Mo}$ -sw values, providing another approach to reconstructing the Mo isotopic composition of ancient oceans (Wen et al., 2011).

### 4.3 Existing problems for the model

The most serious problems associated with this model come from the possibility of errors in estimating the  $\delta^{98}\text{Mo}$  value in RED. Sediments in RED have variable isotopic compositions. To simplify the mass balance model,  $\delta^{98}\text{Mo}$  values for these sediments are usually calculated by subtracting a fractionation of  $0.7\text{‰}$  from the  $\delta^{98}\text{Mo}$ -sw value (Arnold et al., 2004; Kendall et al., 2009). This assumption can cause significant errors in the model results. Moreover, estimating

the Mo input fluxes at a given time can be difficult. In a steady state ocean, the Mo influx is approximately equal to the Mo outflux, making the mass balance model valid. However, modern estimates of Mo influx may not apply to the geologic past. Even today, the riverine Mo concentration and isotopic composition vary by region, climate and even season (Archer and Vance, 2008). In the Precambrian, global temperatures were probably higher than today (Gaucher et al., 2008), which could result in stronger weathering and higher riverine Mo concentrations. However, the low atmospheric oxygen level at that time would have the opposite effect (Canfield, 2005; Holland, 2006). Therefore, further works are needed for accurately running the model.

## 5 Conclusions and future works

In light of our review, we conclude that Mo concentration, Mo/TOC values and Mo isotopic compositions can provide information about local water redox conditions but also quantitative evaluation of the redox state of the global oceans, which is significant for the reconstruction of ancient ocean chemistry. However, our review also indicates that the mechanisms controlling Mo accumulation and isotopic fractionation are complex. This complexity may impart uncertainty to the application of these Mo proxies in the reconstruction of ancient ocean chemistry and particularly global ocean redox state. Therefore, while we believe that Mo proxies can play a major role in quantitative analysis of ancient ocean chemistry, we suggest that they should be used in conjunction with other geochemical proxies.

Future studies of Mo geochemical proxies in the reconstruction of ancient ocean chemistry should focus on the following: (1) the mechanisms of transferring Mo from the water column to the sediments as  $\text{MoS}_4^{2-}$  and subsequent chemical cycling of Mo in the sediments; and (2) the effects of a stratified marine redox structure and spatially heterogeneous ocean chemistry on Mo enrichment and isotopic composition at both local and global scales.

*We thank Cheng-Sheng Jin and Dong-Mei Qi for their valuable discussions. We also thank the two anonymous reviewers for their valuable comments. This research was supported by the National Basic Research Program of China (Grant No. 2013CB955704) and the National Natural Science Foundation of China (Grant No. 41172030).*

- Algeo T J. 2004. Can marine anoxic events draw down the trace element inventory of seawater? *Geology*, 32: 1057
- Algeo T J, Lyons T W. 2006. Mo-total organic carbon covariation in modern anoxic marine environments: Implications for analysis of paleoredox and paleohydrographic conditions. *Paleoceanography*, 21, doi: 10.1029/2004pa001112
- Algeo T J, Maynard J B. 2004. Trace-element behavior and redox facies in core shales of Upper Pennsylvanian Kansas-type cyclothems. *Chem Geol*, 206: 289–318

- Anbar A D. 2004. Molybdenum stable isotopes: Observations, interpretations and directions. *Rev Mineral Geochem*, 55: 429–454
- Anbar A D, Knoll A H. 2002. Proterozoic ocean chemistry and evolution: A bioinorganic bridge? *Science*, 297: 1137–1142
- Anbar A D, Rouxel O. 2007. Metal Stable Isotopes in Paleooceanography. *Annu Rev Earth Planet Sci*, 35: 717–746
- Archer C, Vance D. 2008. The isotopic signature of the global riverine molybdenum flux and anoxia in the ancient oceans. *Nat Geosci*, 1: 597–600
- Arnold G L, Anbar A D, Barling J, Lyons T W. 2004. Molybdenum isotope evidence for widespread anoxia in mid-Proterozoic oceans. *Science*, 304: 87–90
- Arnold G L, Lyons T W, Gordon G W, Anbar A D. 2012. Extreme change in sulfide concentrations in the Black Sea during the Little Ice Age reconstructed using molybdenum isotopes. *Geology*, 40: 595–598
- Baldwin G J, Nägler T F, Greber N D, Turner E C, Kamber B S. 2013. Mo isotopic composition of the mid-Neoproterozoic ocean: An iron formation perspective. *Precambrian Res*, 230: 168–178
- Barling J, Anbar A D. 2004. Molybdenum isotope fractionation during adsorption by manganese oxides. *Earth Planet Sci Lett*, 217: 315–329
- Barling J, Arnold G L, Anbar A D. 2001. Natural mass-dependent variations in the isotopic composition of molybdenum. *Earth Planet Sci Lett*, 193: 447–457
- Bekker A, Holland H D, Wang P L, Rumble D, Stein H J, Hannah J L, Coetzee L L, Beukes N J. 2004. Dating the rise of atmospheric oxygen. *Nature*, 427: 117–120
- Brocks J J. 2005. Building the biomarker tree of life. *Rev Mineral Geochem*, 59: 233–258
- Brumsack H J. 1989. Geochemistry of recent TOC-rich sediments from the Gulf of California and the Black Sea. *Int J Earth Sci Geol Rundschau*, 78: 851–882
- Canfield D E. 1998. A new model for Proterozoic ocean chemistry. *Nature*, 396: 450–453
- Canfield D E. 2005. The early history of atmospheric oxygen: Homage to Robert M. Garrels. *Annu Rev Earth Planet Sci*, 33: 1–36
- Canfield D E, Ngombi-Pemba L, Hammarlund E U, Bengtson S, Chaussidon M, Gauthier-Lafaye F, Meunier A, Riboulleau A, Rollion-Bard C, Rouxel O, Asael D, Pierson-Wickmann A C, Albani A E. 2013. Oxygen dynamics in the aftermath of the Great Oxidation of Earth's atmosphere. *Proc Natl Acad Sci USA*, 110: 16736–16741
- Canfield D E, Thamdrup B. 2009. Towards a consistent classification scheme for geochemical environments, or, why we wish the term 'suboxic' would go away. *Geobiology*, 7: 385–92
- Chen X, Ling H F, Vance D, Shields-Zhou G A, Zhu M, Poulton S W, Och L M, Jiang S Y, Li D, Cremonese L, Archer C. 2015. Rise to modern levels of ocean oxygenation coincided with the Cambrian radiation of animals. *Nat Commun*, 6, doi: 10.1038/ncomms8142
- Collier R W. 1985. Molybdenum in the northeast Pacific Ocean. *Limnol Oceanogr*, 30: 1351–1354
- Czaja A D, Johnson C M, Roden E E, Beard B L, Voegelin A R, Nagler T F, Beukes N J, Wille M. 2012. Evidence for free oxygen in the Neoproterozoic ocean based on coupled iron-molybdenum isotope fractionation. *Geochim Cosmochim Acta*, 86: 118–137
- Dahl T W, Anbar A D, Gordon G W, Rosing M T, Frei R, Canfield D E. 2010a. The behavior of molybdenum and its isotopes across the chemocline and in the sediments of sulfidic Lake Cadagno, Switzerland. *Geochim Cosmochim Acta*, 74: 144–163
- Dahl T W, Canfield D E, Rosing M T, Frei R E, Gordon G W, Knoll A H, Anbar A D. 2011. Molybdenum evidence for expansive sulfidic water masses in ~750 Ma oceans. *Earth Planet Sci Lett*, 311: 264–274
- Dahl T W, Hammarlund E U, Anbar A D, Bond D P G, Gill B C, Gordon G W, Knoll A H, Nielsen A T, Schovsbo N H, Canfield D E. 2010b. Devonian rise in atmospheric oxygen correlated to the radiations of terrestrial plants and large predatory fish. *Proc Natl Acad Sci USA*, 107: 17911–17915
- Duan Y, Anbar A D, Arnold G L, Lyons T W, Gordon G W, Kendall B. 2010. Molybdenum isotope evidence for mild environmental oxygenation before the Great Oxidation Event. *Geochim Cosmochim Acta*, 74: 6655–6668
- Eroglu S, Schoenberg R, Wille M, Beukes N, Taubald H. 2015. Geochemical stratigraphy, sedimentology, and Mo isotope systematics of the ca. 2.58–2.50 Ga-old Transvaal Supergroup carbonate platform, South Africa. *Precambrian Res*, 266: 27–46
- Farquhar J. 2000. Atmospheric influence of Earth's earliest sulfur cycle. *Science*, 289: 756–758
- Feng L, Li C, Huang J, Chang H, Chu X. 2014. A sulfate control on marine mid-depth euxinia on the early Cambrian (ca. 529–521 Ma) Yangtze platform, South China. *Precambrian Res*, 246: 123–133
- Fike D A, Grotzinger J P, Pratt L M, Summons R E. 2006. Oxidation of the Ediacaran ocean. *Nature*, 444: 744–747
- Gaucher E A, Govindarajan S, Ganesh O K. 2008. Palaeotemperature trend for Precambrian life inferred from resurrected proteins. *Nature*, 451: 704–707
- Gilleaudeau G J, Kah L C. 2013. Oceanic molybdenum drawdown by epeiric sea expansion in the Mesoproterozoic. *Chem Geol*, 356: 21–37
- Goldberg T, Archer C, Vance D, Poulton S W. 2009. Mo isotope fractionation during adsorption to Fe (oxyhydr) oxides. *Geochim Cosmochim Acta*, 73: 6502–6516
- Goldberg T, Archer C, Vance D, Thamdrup B, McAnena A, Poulton S W. 2012. Controls on Mo isotope fractionations in a Mn-rich anoxic marine sediment, Gullmar Fjord, Sweden. *Chem Geol*, 296–297: 73–82
- Goldberg T, Gordon G, Izon G, Archer C, Pearce C R, McManus J, Anbar A D, Rehkämper M. 2013. Resolution of inter-laboratory discrepancies in Mo isotope data: an intercalibration. *J Ann Atom Spectrom*, 28: 724–735
- Goldberg T, Strauss H, Guo Q, Liu C. 2007. Reconstructing marine redox conditions for the Early Cambrian Yangtze Platform: Evidence from biogenic sulphur and organic carbon isotopes. *Paleogeogr Paleoclimatol Paleoeconol*, 254: 175–193
- Gordon G W, Lyons T W, Arnold G L, Roe J, Sageman B B, Anbar A D. 2009. When do black shales tell molybdenum isotope tales? *Geology*, 37: 535–538
- Greber N D, Hofmann B A, Voegelin A R, Villa I M, Nägler T F. 2011. Mo isotope composition in Mo-rich high- and low-*T* hydrothermal systems from the Swiss Alps. *Geochim Cosmochim Acta*, 75: 6600–6609
- Hannah J L, Stein H J, Wieser M E, de Laeter J R, Varner M D. 2007. Molybdenum isotope variations in molybdenite: Vapor transport and Rayleigh fractionation of Mo. *Geology*, 35: 703–706
- Hansel C M, Zeiner C A, Santelli C M, Webb S M. 2012. Mn(II) oxidation by an ascomycete fungus is linked to superoxide production during asexual reproduction. *Proc Natl Acad Sci USA*, 109: 12621–12625
- Helz G R, Bura-Nakić E, Mikac N, Ciglencić I. 2011. New model for molybdenum behavior in euxinic waters. *Chem Geol*, 284: 323–332
- Helz G R, Miller C V, Charnock J M, Mosselmans J F W, Patrick R A D, Garner C D, Vaughan D J. 1996. Mechanism of molybdenum removal from the sea and its concentration in black shales: EXAFS evidence. *Geochim Cosmochim Acta*, 60: 3631–3642
- Herrmann A D, Kendall B, Algeo T J, Gordon G W, Wasylenko L E, Anbar A D. 2012. Anomalous molybdenum isotope trends in Upper Pennsylvanian euxinic facies: Significance for use of  $\delta^{98}\text{Mo}$  as a global marine redox proxy. *Chem Geol*, 324–325: 87–98
- Hoffman P F. 1998. A Neoproterozoic Snowball Earth. *Science*, 281: 1342–1346
- Holland H D. 2006. The oxygenation of the atmosphere and oceans. *Philos Trans R Soc B-Biol Sci*, 361: 903–915
- Kah L C, Lyons T W, Frank T D. 2004. Low marine sulphate and protracted oxygenation of the Proterozoic biosphere. *Nature*, 431: 834–838
- Kasting J F. 2001. Earth history. The rise of atmospheric oxygen. *Science*, 293: 819–820
- Kendall B, Creaser R A, Gordon G W, Anbar A D. 2009. Re-Os and Mo isotope systematics of black shales from the Middle Proterozoic Velkerri and Wollgorang Formations, McArthur Basin, northern Australia. *Geochim Cosmochim Acta*, 73: 2534–2558
- Kendall B, Gordon G W, Poulton S W, Anbar A D. 2011. Molybdenum isotope constraints on the extent of late Paleoproterozoic ocean euxinia. *Earth Planet Sci Lett*, 307: 450–460
- Kendall B, Komiyama T, Lyons T W, Bates S M, Gordon G W, Romaniello S J, Jiang G Q, Creaser R A, Xiao S H, McFadden K, Sawaki Y, Tahata

- M, Shu D G, Han J, Li Y, Chu X L, Anbar A D. 2015. Uranium and molybdenum isotope evidence for an episode of widespread ocean oxygenation during the late Ediacaran Period. *Geochim Cosmochim Acta*, 156: 173–193
- Kowalski N, Dellwig O, Beck M, Grawe U, Neubert N, Nagler T F, Badewien T H, Brumsack H J, van Beusekom J E E, Bottcher M E. 2013. Pelagic molybdenum concentration anomalies and the impact of sediment resuspension on the molybdenum budget in two tidal systems of the North Sea. *Geochim Cosmochim Acta*, 119: 198–211
- Kump L R. 2008. The rise of atmospheric oxygen. *Nature*, 451: 277–278
- Kump L R, Seyfried W E. 2005. Hydrothermal Fe fluxes during the Precambrian: Effect of low oceanic sulfate concentrations and low hydrostatic pressure on the composition of black smokers. *Earth Planet Sci Lett*, 235: 654–662
- Kurzweil F, Wille M, Schoenberg R, Taubald H, Van Kranendonk M J. 2015. Continuously increasing  $\delta^{98}\text{Mo}$  values in Neoproterozoic black shales and iron formations from the Hamersley Basin. *Geochim Cosmochim Acta*, 164: 523–542
- Lehmann B, Nagler T F, Holland H D, Wille M, Mao J, Pan J, Ma D, Dulski P. 2007. Highly metalliferous carbonaceous shale and Early Cambrian seawater. *Geology*, 35: 403–406
- Li C, Love G D, Lyons T W, Fike D A, Sessions A L, Chu X. 2010. A stratified redox model for the Ediacaran ocean. *Science*, 328: 80–83
- Li C, Love G D, Lyons T W, Scott C T, Feng L, Huang J, Chang H, Zhang Q, Chu X. 2012. Evidence for a redox stratified Cryogenian marine basin, Datangpo Formation, South China. *Earth Planet Sci Lett*, 331–332: 246–256
- Li C, Planavsky N J, Love G D, Reinhard C T, Hardisty D, Feng L J, Bates S M, Huang J, Zhang Q R, Chu X L, Lyons T W. 2015. Marine redox conditions in the middle Proterozoic ocean and isotopic constraints on authigenic carbonate formation: Insights from the Chuanlinggou Formation, Yanshan Basin, North China. *Geochim Cosmochim Acta*, 150: 90–105
- Li Z X, Bogdanova S V, Collins A S, Davidson A, De Waele B, Ernst R E, Fitzsimons I C W, Fuck R A, Gladkochub D P, Jacobs J, Karlstrom K E, Lu S, Natapov L M, Pease V, Pisarevsky S A, Thrane K, Verikovsky V. 2008. Assembly, configuration, and break-up history of Rodinia: A synthesis. *Precambrian Res*, 160: 179–210
- Liermann L J, Guynn R L, Anbar A, Brantley S L. 2005. Production of a molybdophore during metal-targeted dissolution of silicates by soil bacteria. *Chem Geol*, 220: 285–302
- Lloyd S J, Marengo P J, Hagadorn J W, Lyons T W, Kaufman A J, Sour-Tovar F, Corsetti F A. 2012. Sustained low marine sulfate concentrations from the Neoproterozoic to the Cambrian: Insights from carbonates of northwestern Mexico and eastern California. *Earth Planet Sci Lett*, 339–340: 79–94
- Lyons T W, Anbar A D, Severmann S, Scott C, Gill B C. 2009. Tracking euxinia in the ancient ocean: A multiproxy perspective and Proterozoic case study. *Annu Rev Earth Planet Sci*, 37: 507–534
- McFadden K A, Huang J, Chu X, Jiang G, Kaufman A J, Zhou C, Yuan X, Xiao S. 2008. Pulsed oxidation and biological evolution in the Ediacaran Doushantuo Formation. *Proc Natl Acad Sci USA*, 105: 3197–202
- McManus J, Nagler T F, Siebert C, Wheat C G, Hammond D E. 2002. Oceanic molybdenum isotope fractionation: Diagenesis and hydrothermal ridge-flank alteration. *Geochem Geophys Geosyst*, 3: 1–9
- Metz S, Trefry J H. 2000. Chemical and mineralogical influences on concentrations of trace metals in hydrothermal fluids. *Geochim Cosmochim Acta*, 64: 2267–2279
- Miller C A, Peucker-Ehrenbrink B, Walker B D, Marcantonio F. 2011. Re-assessing the surface cycling of molybdenum and rhenium. *Geochim Cosmochim Acta*, 75: 7146–7179
- Morel F M, Price N M. 2003. The biogeochemical cycles of trace metals in the oceans. *Science*, 300: 944–947
- Morford J L, Russell A D, Emerson S. 2001. Trace metal evidence for changes in the redox environment associated with the transition from terrigenous clay to diatomaceous sediment, Saanich Inlet, BC. *Mar Geol*, 174: 355–369
- Nagler T F, Neubert N, Böttcher M E, Dellwig O, Schnetger B. 2011. Molybdenum isotope fractionation in pelagic euxinia: Evidence from the modern Black and Baltic Seas. *Chem Geol*, 289: 1–11
- Nameroff T J, Balistrieri L S, Murray J W. 2002. Suboxic trace metal geochemistry in the eastern tropical North Pacific. *Geochim Cosmochim Acta*, 66: 1139–1158
- Neubert N, Heri A R, Voegelin A R, Nagler T F, Schlunegger F, Villa I M. 2011. The molybdenum isotopic composition in river water: Constraints from small catchments. *Earth Planet Sci Lett*, 304: 180–190
- Neubert N, Nagler T F, Böttcher M E. 2008. Sulfidity controls molybdenum isotope fractionation into euxinic sediments: Evidence from the modern Black Sea. *Geology*, 36: 775–778
- Och L M, Shields-Zhou G A. 2012. The Neoproterozoic oxygenation event: Environmental perturbations and biogeochemical cycling. *Earth-Sci Rev*, 110: 26–57
- Pearce C R, Cohen A S, Coe A L, Burton K W. 2008. Molybdenum isotope evidence for global ocean anoxia coupled with perturbations to the carbon cycle during the Early Jurassic. *Geology*, 36: 231–234
- Planavsky N J, Asael D, Hofmann A, Reinhard C T, Lalonde S V, Knudsen A, Wang X, Ossa Ossa F, Pecoits E, Smith A J B, Beukes N J, Bekker A, Johnson T M, Konhauser K O, Lyons T W, Rouxel O J. 2014a. Evidence for oxygenic photosynthesis half a billion years before the Great Oxidation Event. *Nat Geosci*, 7: 283–286
- Planavsky N J, Reinhard C T, Wang X, Thomson D, McGoldrick P, Rainbird R H, Johnson T, Fischer W W, Lyons T W. 2014b. Low mid-Proterozoic atmospheric oxygen levels and the delayed rise of animals. *Science*, 346: 635–638
- Poulson R L, McManus J, Severmann S, Berelson W M. 2009. Molybdenum behavior during early diagenesis: Insights from Mo isotopes. *Geochem Geophys Geosyst*, 10, doi: 10.1029/2008GC002180
- Poulson R L, Siebert C, McManus J, Berelson W M. 2006. Authigenic molybdenum isotope signatures in marine sediments. *Geology*, 34: 617–620
- Poulton S W, Fralick P W, Canfield D E. 2010. Spatial variability in oceanic redox structure 1.8 billion years ago. *Nat Geosci*, 3: 486–490
- Proemse B C, Grasby S E, Wieser M E, Mayer B, Beauchamp B. 2013. Molybdenum isotopic evidence for oxic marine conditions during the latest Permian extinction. *Geology*, 41: 967–970
- Rahaman W, Singh S K, Raghav S. 2010. Dissolved Mo and U in rivers and estuaries of India: Implication to geochemistry of redox sensitive elements and their marine budgets. *Chem Geol*, 278: 160–172
- Reinhard C T, Planavsky N J, Robbins L J, Partin C A, Gill B C, Lalonde S V, Bekker A, Konhauser K O, Lyons T W. 2013. Proterozoic ocean redox and biogeochemical stasis. *Proc Natl Acad Sci USA*, 110: 5357–5362
- Reinhard C T, Raiswell R, Scott C, Anbar A D, Lyons T W. 2009. A late Archean sulfidic sea stimulated by early oxidative weathering of the continents. *Science*, 326: 713–716.
- Reitz A, Wille M, Nagler T, Delange G. 2007. Atypical Mo isotope signatures in eastern Mediterranean sediments. *Chem Geol*, 245: 1–8
- Rouxel O J, Bekker A, Edwards K J. 2005. Iron isotope constraints on the Archean and Paleoproterozoic ocean redox state. *Science*, 307: 1088–1091
- Sahoo S K, Planavsky N J, Kendall B, Wang X, Shi X, Scott C, Anbar A D, Lyons T W, Jiang G. 2012. Ocean oxygenation in the wake of the Marinoan glaciation. *Nature*, 489: 546–549
- Scott C, Lyons T W. 2012. Contrasting molybdenum cycling and isotopic properties in euxinic versus non-euxinic sediments and sedimentary rocks: Refining the paleoproxies. *Chem Geol*, 324: 19–27
- Scott C, Lyons T W, Bekker A, Shen Y, Poulton S W, Chu X, Anbar A D. 2008. Tracing the stepwise oxygenation of the Proterozoic ocean. *Nature*, 452: 456–459
- Siebert C, Kramers J D, Meisel T, Morel P, Nagler T F. 2005. PGE, Re-Os, and Mo isotope systematics in Archean and early Proterozoic sedimentary systems as proxies for redox conditions of the early Earth. *Geochim Cosmochim Acta*, 69: 1787–1801
- Siebert C, Nagler T F, von Blanckenburg F, Kramers J D. 2003. Molybdenum isotope records as a potential new proxy for paleoceanography. *Earth Planet Sci Lett*, 211: 159–171
- Siebert C, Nagler T F, Kramers J D. 2001. Determination of molybdenum isotope fractionation by double-spoke multicollector inductively cou-

- pled plasma mass spectrometry. *Geochem Geophys Geosyst*, 2, doi: 10.1029/2000GC000124
- Slack J F, Cannon W F. 2009. Extraterrestrial demise of banded iron formations 1.85 billion years ago. *Geology*, 37: 1011–1014
- Slack J F, Grenne T, Bekker A, Rouxel O J, Lindberg P A. 2007. Suboxic deep seawater in the late Paleoproterozoic: Evidence from hematitic chert and iron formation related to seafloor-hydrothermal sulfide deposits, central Arizona, USA. *Earth Planet Sci Lett*, 255: 243–256
- Takahashi S, Yamasaki S-i, Ogawa Y, Kimura K, Kaiho K, Yoshida T, Tsuchiya N. 2014. Bioessential element-depleted ocean following the euxinic maximum of the end-Permian mass extinction. *Earth Planet Sci Lett*, 393: 94–104
- Tossell J A. 2005. Calculating the partitioning of the isotopes of Mo between oxidic and sulfidic species in aqueous solution. *Geochim Cosmochim Acta*, 69: 2981–2993
- Turekian K K, Holland H D. 2013. *Treatise on Geochemistry*. 2nd ed. New York: Elsevier Science
- Voegelin A R, Nägler T F, Beukes N J, Lacassie J P. 2010. Molybdenum isotopes in late Archean carbonate rocks: Implications for early Earth oxygenation. *Precambrian Res*, 182: 70–82
- Voegelin A R, Nägler T F, Samankassou E, Villa I M. 2009. Molybdenum isotopic composition of modern and Carboniferous carbonates. *Chem Geol*, 265: 488–498
- Voegelin A R, Pettke T, Greber N D, von Niederhäusern B, Nägler T F. 2014. Magma differentiation fractionates Mo isotope ratios: Evidence from the Kos Plateau Tuff (Aegean Arc). *Lithos*, 190-191: 440–448
- Wang D, Aller R C, Sañudo-Wilhelmy S A. 2011. Redox speciation and early diagenetic behavior of dissolved molybdenum in sulfidic muds. *Mar Chem*, 125: 101–107
- Wasylenki L E, Rolfe B A, Weeks C L, Spiro T G, Anbar A D. 2008. Experimental investigation of the effects of temperature and ionic strength on Mo isotope fractionation during adsorption to manganese oxides. *Geochim Cosmochim Acta*, 72: 5997–6005
- Wen H, Carignan J, Zhang Y, Fan H, Cloquet C, Liu S. 2011. Molybdenum isotopic records across the Precambrian-Cambrian boundary. *Geology*, 39: 775–778
- Wen H, Fan H, Zhang Y, Cloquet C, Carignan J. 2015. Reconstruction of early Cambrian ocean chemistry from Mo isotopes. *Geochim Cosmochim Acta*, 164: 1–16
- Wheat C G, Mottl M J, Rudnicki M. 2002. Trace element and REE composition of a low-temperature ridge-flank hydrothermal spring. *Geochim Cosmochim Acta*, 66: 3693–3705
- Wille M, Kramers J D, Nägler T F, Beukes N J, Schröder S, Meisel T, Lacassie J P, Voegelin A R. 2007. Evidence for a gradual rise of oxygen between 2.6 and 2.5 Ga from Mo isotopes and Re-PGE signatures in shales. *Geochim Cosmochim Acta*, 71: 2417–2435
- Wille M, Nägler T F, Lehmann B, Schröder S, Kramers J D. 2008. Hydrogen sulphide release to surface waters at the Precambrian/Cambrian boundary. *Nature*, 453: 767–769
- Wille M, Nebel O, Van Kranendonk M J, Schoenberg R, Kleinhanns I C, Ellwood M J. 2013. Mo-Cr isotope evidence for a reducing Archean atmosphere in 3.46–2.76 Ga black shales from the Pilbara, Western Australia. *Chem Geol*, 340: 68–76
- Xu L, Lehmann B, Mao J, Nägler T F, Neubert N, Böttcher M E, Escher P. 2012. Mo isotope and trace element patterns of Lower Cambrian black shales in South China: Multi-proxy constraints on the paleoenvironment. *Chem Geol*, 318-319: 45–59
- Zerkle A L, Scheiderich K, Maresca J A, Liermann L J, Brantley S L. 2011. Molybdenum isotope fractionation by cyanobacterial assimilation during nitrate utilization and N<sub>2</sub> fixation. *Geobiology*, 9: 94–106